Supplementary Information

Second-phase Induced Fluorescence Quenching in Non-equivalent Substituted Red Phosphors

Jun Chen, [a] XianfengYang,[c] Chunyan Jiang,[a] Yunfeng Wang, *[ab] Lei Zhou*[a] and Mingmei Wu*[a]

[a] School of Chemistry/School of Marine Science/School of Chemical Engineering and Technology, Sun Yat-Sen University, Guangzhou 510275/Zhuhai 519082, P. R. China

[b] School of Information Engineering, Nanyang Institute of Technology, Nanyang 473004, P. R. China

[c] Analytical and Testing Center, South China University of Technology, Guangzhou, 510640, P. R. China

* Corresponding authors. Email addresses: ceswmm@mail.sysu.edu.cn (M. M. Wu); zhoul8@mail.sysu.edu.cn (L. Zhou); wangyunfeng@nyist.edu.cn (Yunfeng Wang)

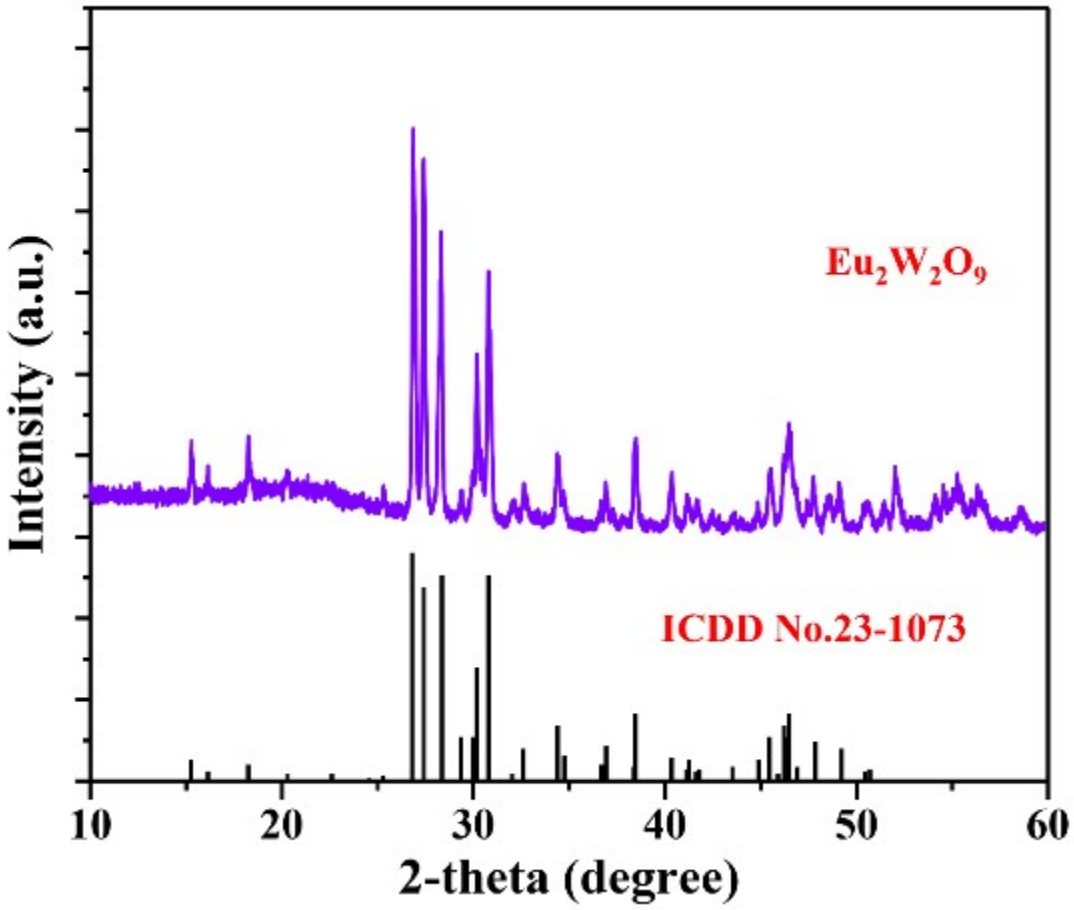

Fig. S1 XRD pattern and standard card of the as-prepared $Eu_2W_2O_9$.

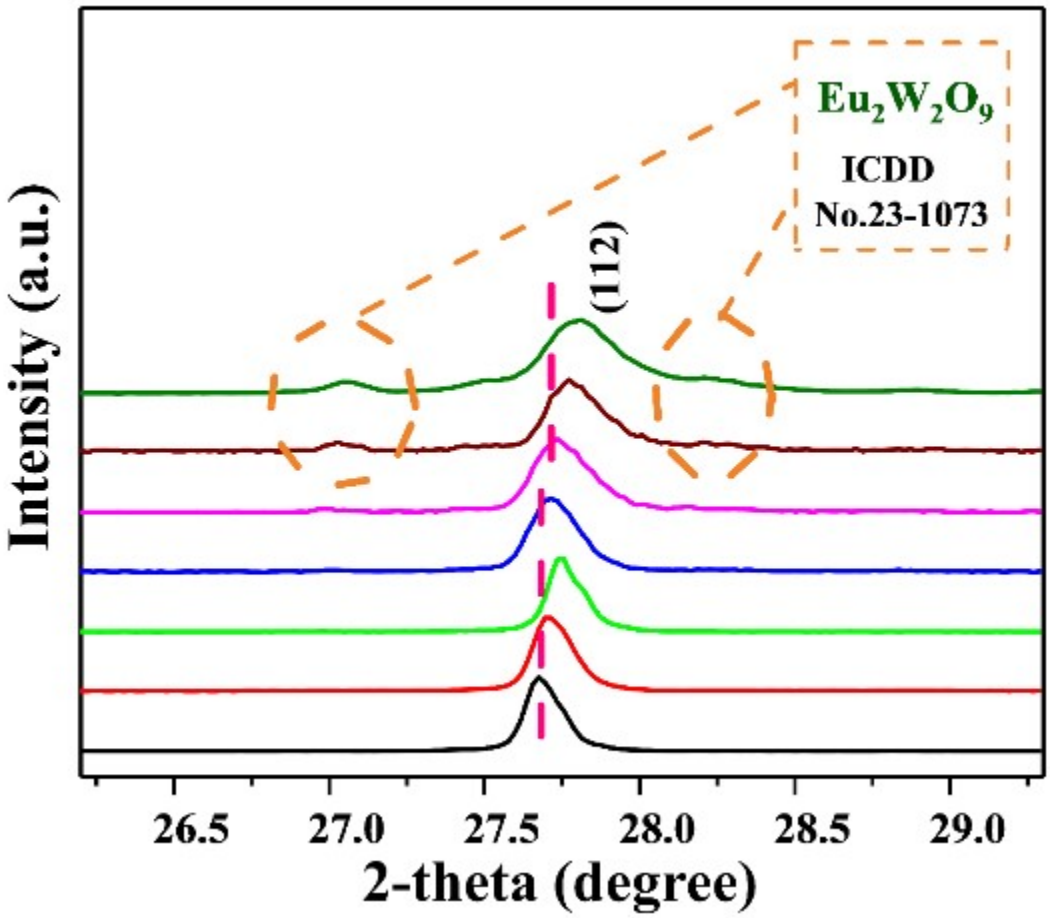

Fig. S2 Magnified XRD patterns with the range of 26.2-29.3°.

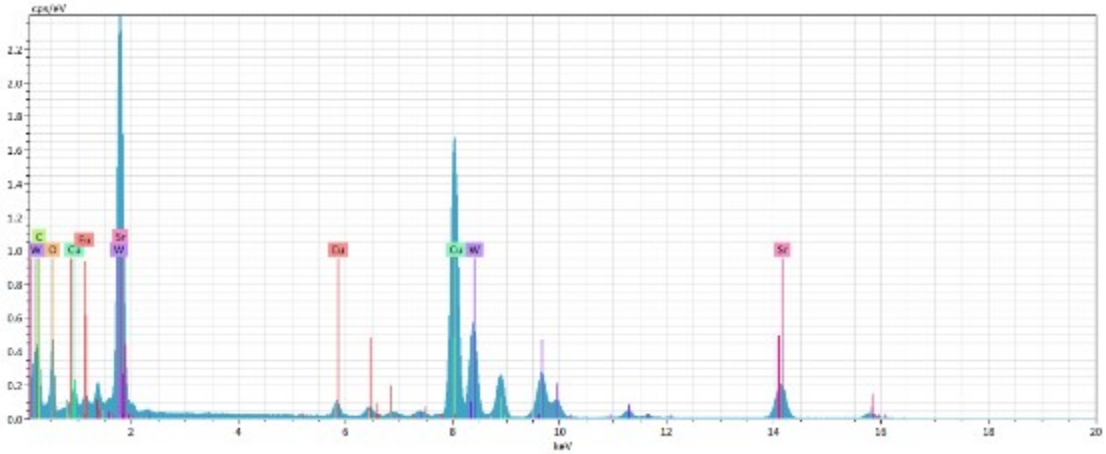

Fig. S3 EDX spectrum of $SrWO_4$:20%Eu^{3+}, the scanning point shows matching elements including Sr, W, Eu, and O.

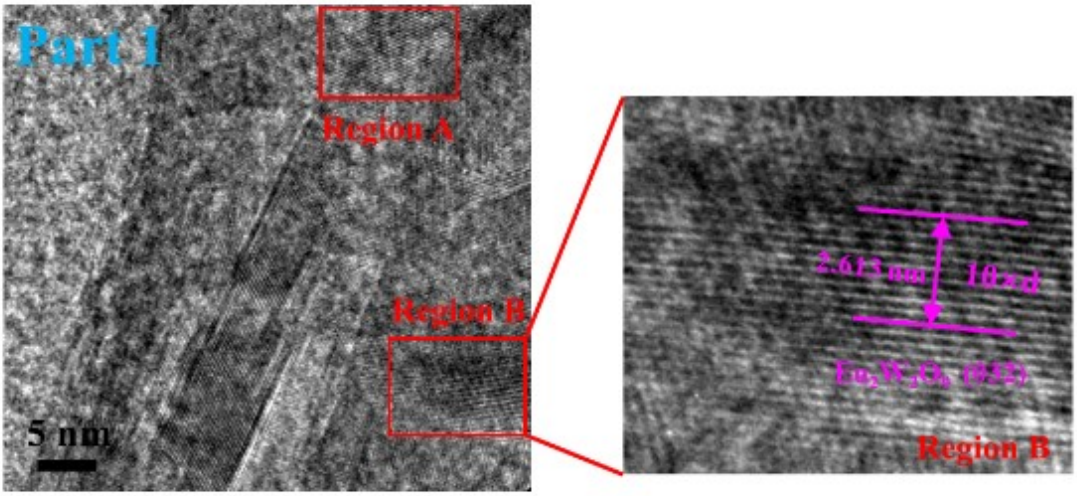

Fig. S4 HR-TEM image of region A and B in part 1, demonstrating the monoclinic crystalline $Eu_2W_2O_9$ possessing lattice fringes of 0.2613 nm, which corresponds to the (032) crystallographic planes.

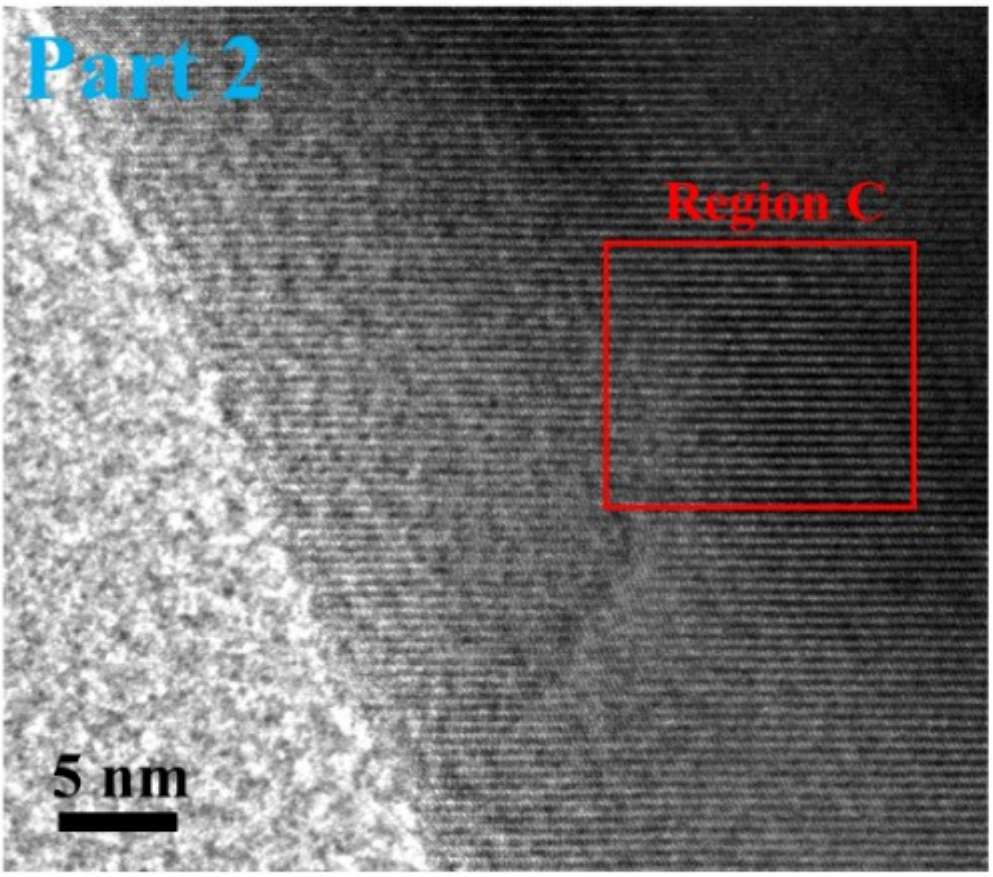

Fig. S5 The TEM image of region C in part 2, demonstrating the typically tetragonal crystalline $SrWO_4$ host lattice with the fringe of 0.4958nm, which corresponds to the crystallographic plane of (101).

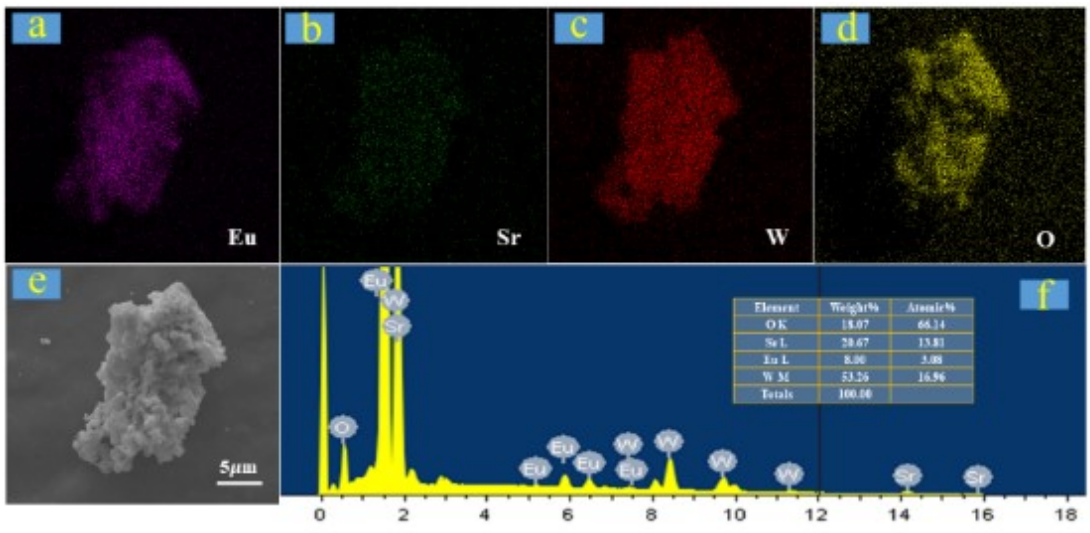

Fig. S6 (a)-(c) Elemental mapping, (e) SEM image, and (f) EDS of the $SrWO_4$:20%Eu^{3+} phosphor, the measurement results indicate the consistent atomic ratios of elementary composition in the as-prepared sample.

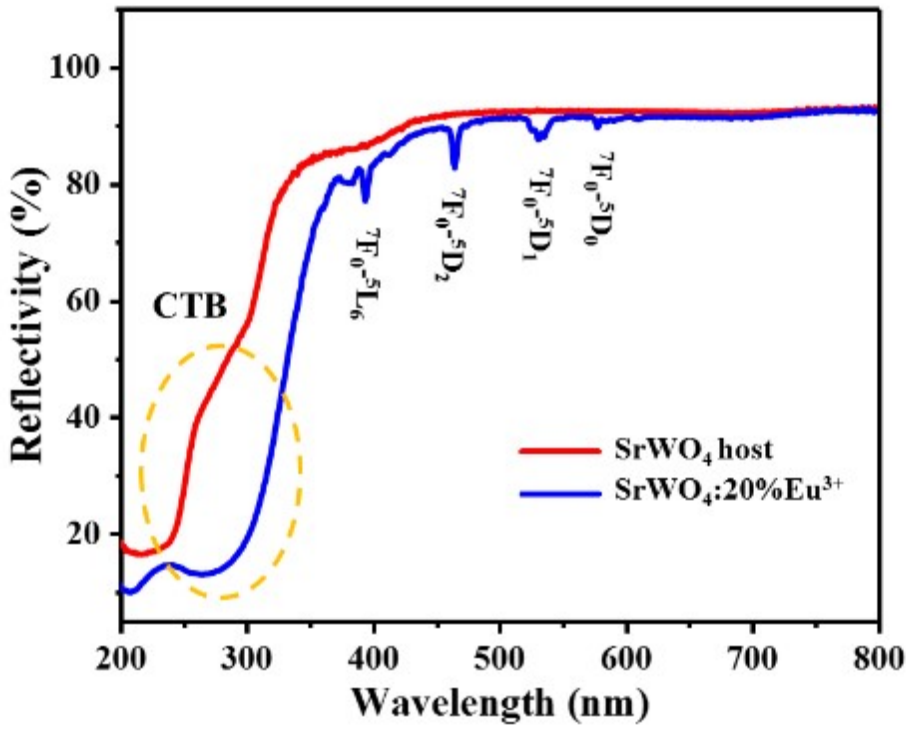

Fig. S7 The diffuse reflection spectra of un-doped and 20%Eu^{3+}-doped $SrWO_4$ sample.

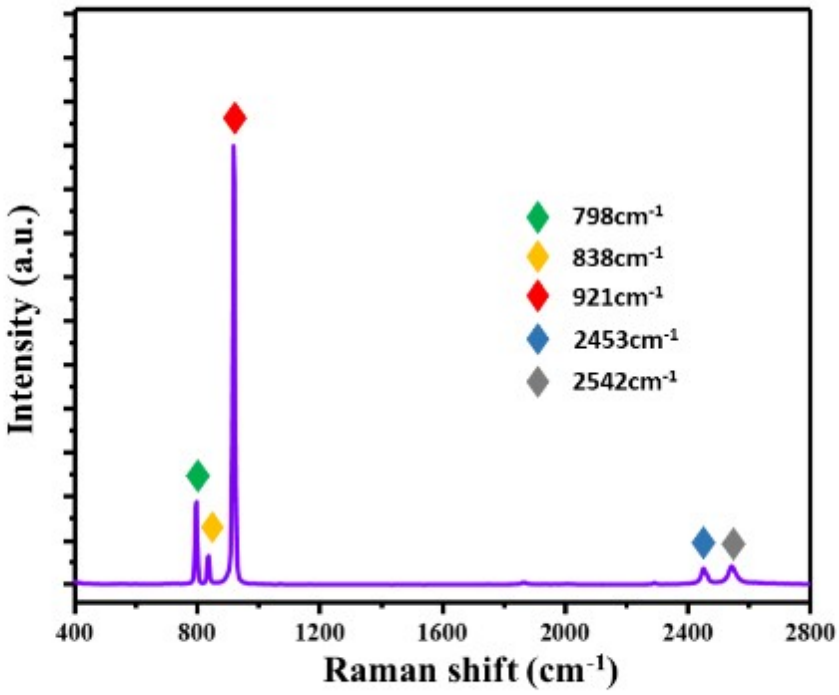

Fig. S8 Raman spectrum of the as-prepared $SrWO_4$:20%Eu^{3+} phosphor, which demonstrates the host lattice with the largest phonon threshold of 921 cm^{-1}.

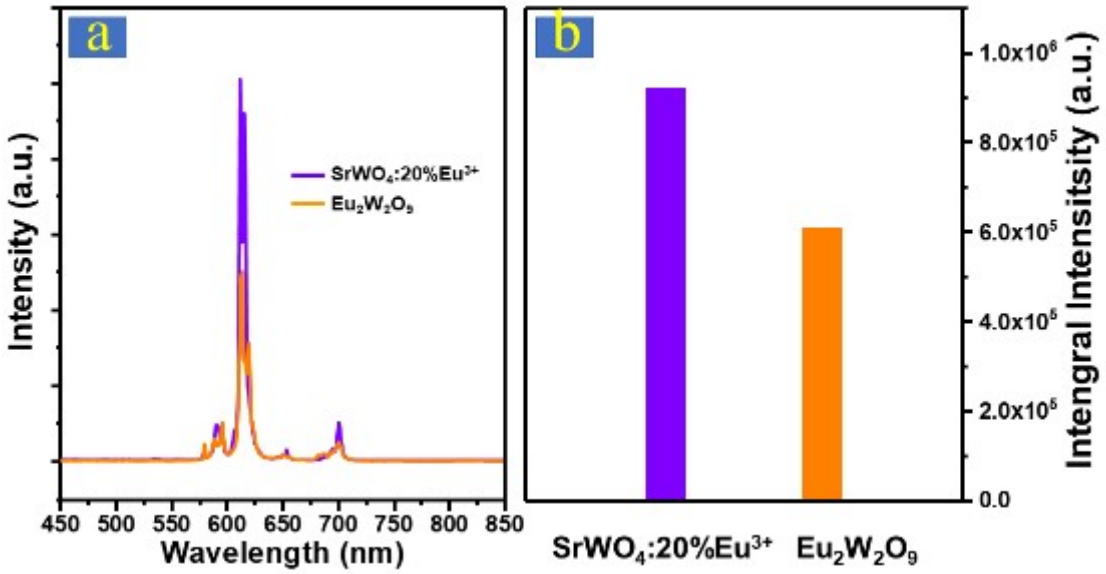

Fig. S9 the emission lines and histogram of integral intensity on as-prepared $SrWO_4$:20%Eu^{3+} and $Eu_2W_2O_9$ samples under 394 nm excitation.

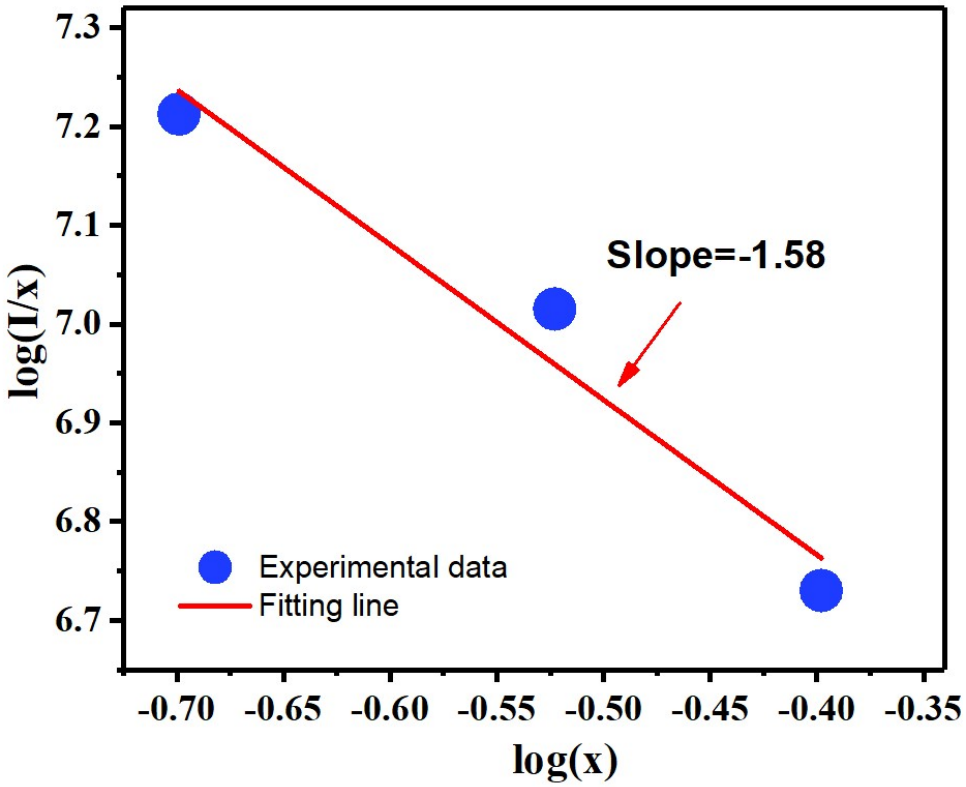

Fig. S10 plot of log(I/x) vs. log(x) for the as-prepared $SrWO_4:xEu^{3+}$ phosphor, x = 20%, 30%, and 40%.

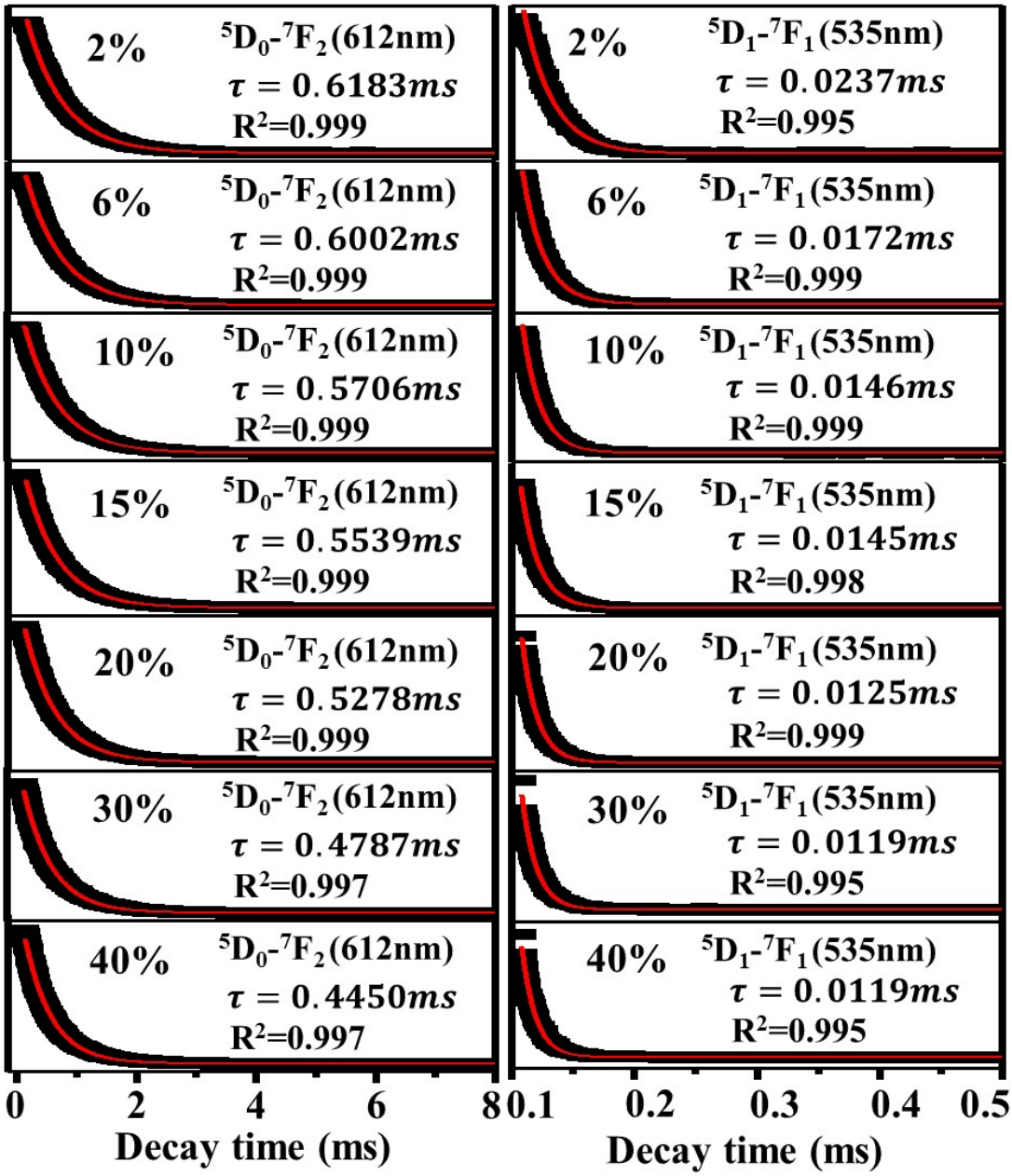

Fig. S11 The decay curves with first order exponential fitting of $^5D_0 \rightarrow ^7F_2$ transition (λ_{em} = 612 nm) and $^5D_1 \rightarrow ^7F_1$ transition (λ_{em} = 535 nm) in $SrWO_4$: $x$$Eu^{3+}$ phosphors under 394 nm excitation.

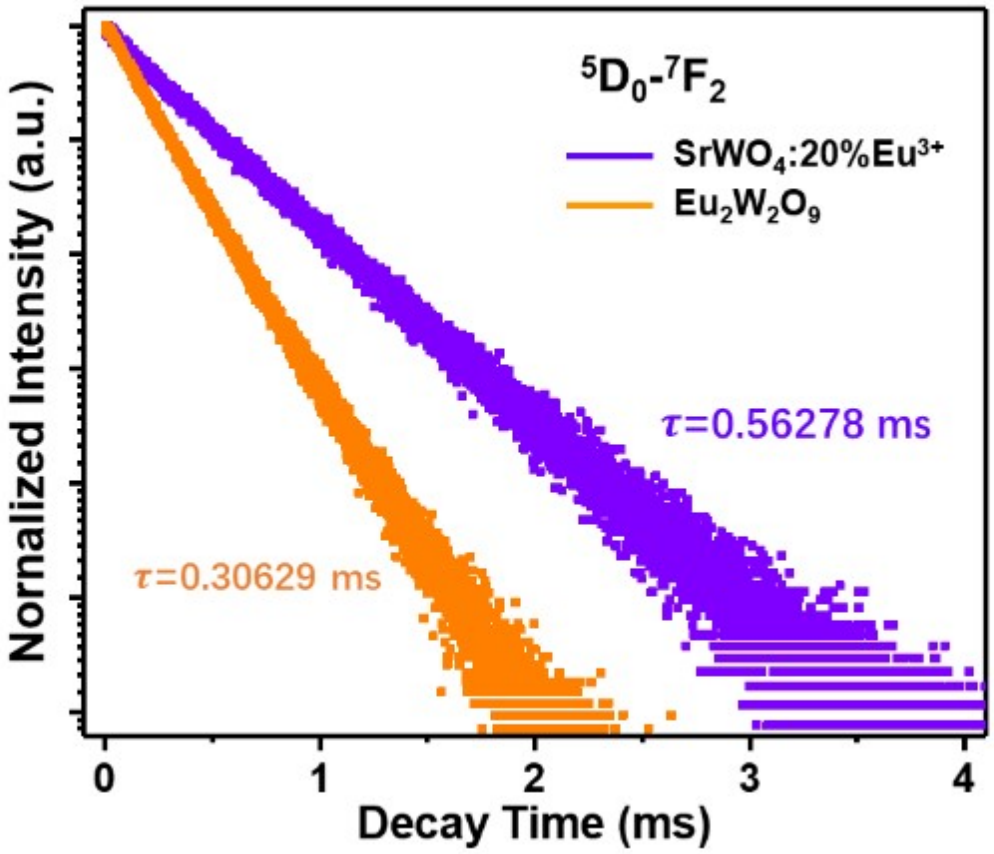

Fig. S12 The decay curves of $^5D_0 \rightarrow {}^7F_2$ transition (λ_{em} = 612 nm) in $SrWO_4$: 20%Eu^{3+} and $Eu_2W_2O_9$ phosphors under 394 nm excitation.

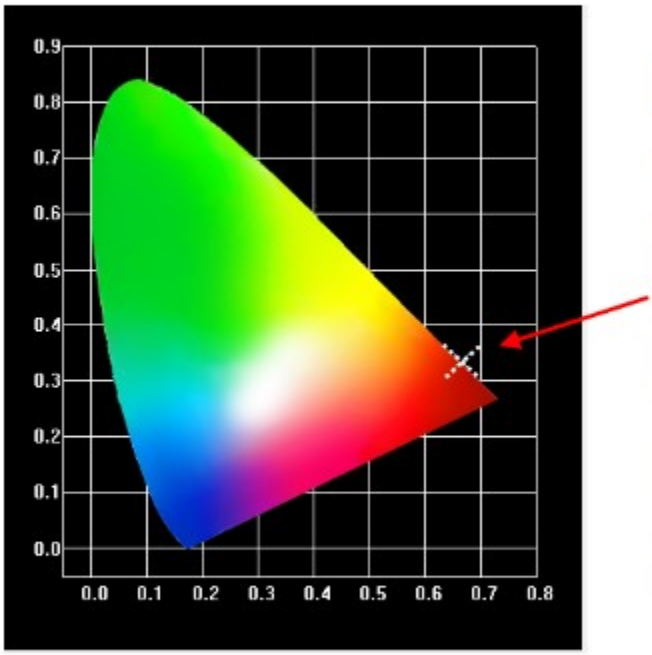

Temp	x	y
300K	0.664	0.335
325K	0.664	0.335
350K	0.664	0.336
375K	0.662	0.337
400K	0.662	0.337
425K	0.661	0.339
450K	0.659	0.340
475K	0.658	0.341
500K	0.655	0.344

Fig. S13 The CIE chromaticity coordinates of $SrWO_4$: 20%Eu^{3+} with the varying temperature range of 300-500 K, which displaying stable emitting colour in high temperature.

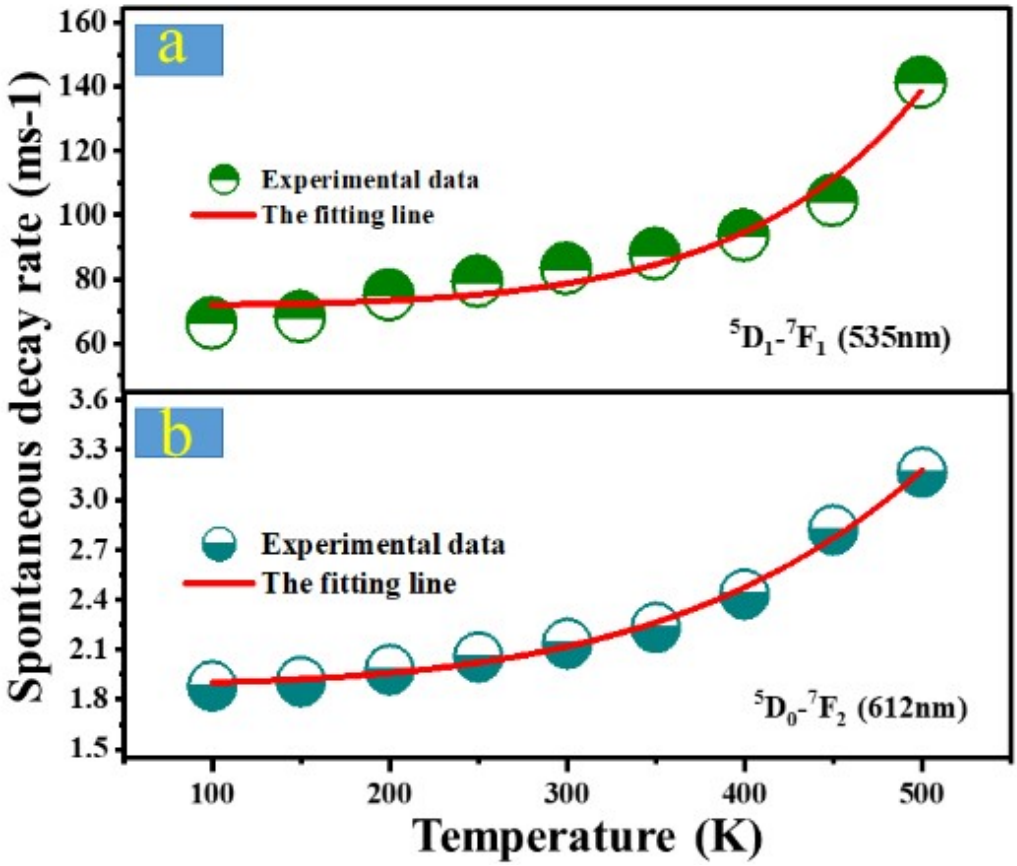

Fig. S14 Temperature-dependent spontaneous decay rate of (a) $^5D_1 \rightarrow ^7F_1$ transition (λ_{em}=535 nm) and (c) $^5D_0 \rightarrow ^7F_2$ transition (λ_{em}=612 nm) in $SrWO_4$: 20%Eu^{3+} sample.

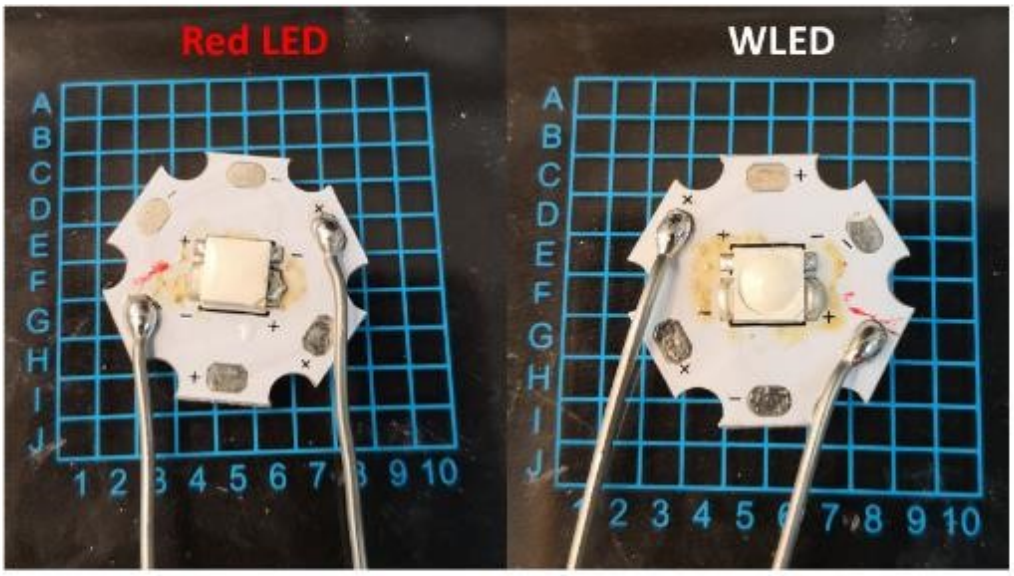

Fig. S15 The as-encapsulated red LED and WLED device by assembling $SrWO_4$:20%Eu^{3+} YGAB: Tb^{3+}, BAM: Eu^{2+} phosphors and near-UV 377nm LED chip.

Traditional concentration quenching mechanism

The concentration quenching mechanism can be calculated by the decrease with the increasing rare-earth doping concentration. The relation between the emission intensity and Eu^{3+} doping concentration is analyzed by the following expression:[1]

$$\log\left(\frac{I}{x}\right) = -\frac{s}{d}\log(x) + log(f)$$

where I represents the emission intensity, x represents the Eu^{3+} concentration. s=6 is associated with dipole-dipole interaction, s=8 is associated with dipole-quadrupole interaction, s=10 is associated with quadrupole-quadrupole interaction. d represents the dimension of compounds, the d value is 3 in general due to the energy transfer of Eu^{3+} in the large-scale micrometer material. f is a constant which is independent of doping concentration. By rough calculation in Fig. S2, the slope of the fitting line is around -1.58, s is determined to be 4.74 approximating to 6. It illustrates the dipole-dipole interaction dominates in the concentration quenching mechanism of $SrWO_4$:xEu^{3+} phosphors.

The colour purity

The colour purity of all $SrWO_4$:xEu^{3+} samples are calculated by the following equation: [1]

$$colour\ purity = \frac{\sqrt{(x - x_i)^2 - (y - y_i)^2}}{\sqrt{(x_d - x_i)^2 - (y_d - y_i)^2}} \times 100\%$$

where (x, y), (x_d, y_d) and (x_i, y_i) are the CIE coordinates of the as-prepared sample, dominant wavelength and white illumination, respectively.

Thermal activation energy

To further understand the quenching behaviour of $SrWO_4$: Eu^{3+} phosphors, the thermal activation energy can be figure out by using the following equation to fit the data of emission intensity:[1]

$$I = \frac{I_0}{1 + \alpha exp(-\Delta E/kT)}$$

where I_0 represents the emission intensity constant, α represents a rate constant on thermally activated escape, ΔE represents the required thermal activation energy on generating temperature quenching, k represents the Boltzmann constant, and T represents the thermodynamic temperature, respectively. From the fitting result in top right corner of Fig. 10, thermal activation energy of $SrWO_4$: 20%Eu^{3+} is 0.27 eV, which is higher than the previous reports, for example, $NaBiF_4$:Eu^{3+} (0.24 eV), $Li_3Gd_3Te_2O_{12}$:Eu^{3+} (0.22 eV), $K_2Gd(PO_4)(WO_4)$:Eu^{3+} (0.19 eV) and $Ba_6Gd_2Ti_4O_{17}$: Eu^{3+}(0.144 eV).[2-5]

The spontaneous decay rates

Based on the multi-phonon relaxation theory, the total spontaneous decay rates (SDRs) of $^5D_1$ and $^5D_0$ can be written as follows:[6]

$$W_{Total} = W_R + W_{NR}(0)(1 - exp(-\hbar\omega/kT))^{-\Delta E/\hbar\omega}$$

where W_{Total} is the total SDR, W_R is the radiative transition rate, $W_{NR}(0)$ is the non-radiative transition rate at 0K, $\hbar\omega$ is the average phonon energy of host material, and ΔE is the energy gap dependence of the transfer probability. By fitting, it is calculated that $W_R = 68.94\ ms^{-1}$ and $W_{NR}(0) = 3.07\ ms^{-1}$ for $^5D_1$-$^7F_1$, $W_R = 1.86\ ms^{-1}$ and $W_{NR}(0) = 0.04\ ms^{-1}$ for $^5D_0$-$^7F_2$, the $W_{NR}(0)$ of $^5D_0$-$^7F_2$ is much smaller than that of $^5D_1$-$^7F_1$. This obvious difference originates from the small gap between $^5D_1$ to $^5D_0$ energy level and the serious phonon-assisted process.

References

1 H. Guo, X. Huang, Y. Zeng, *J. Alloy. Compd.*, 2018, **741**, 300-306.

2 P. Du, X. Huang, J. S. Yu, *Chem. Eng. J.*, 2018, **337**, 91-100.

3 X. Huang, B. Li, H. Guo, *Ceram. Int.*, 2017, **43**, 10566-10571.

4 H. Deng, Z. Gao, N. Xue, J. H. Jeong, R. Yu, *J. Lumin.*, 2017, **192**, 684-689.

5 J. Li, Q. Liang, Y. Cao, J. Yan, J. Zhou, Y. Xu, L. Dolgov, Y. Meng, J. Shi, M. Wu, *ACS Appl. Mater. Interfaces*, 2018, **10**, 41479-41486.

6 Y. Wang, W. Xu, S. Cui, S. Xu, Z. Yin, H. Song, P. Zhou, X. Liu, L. Xu, H. Cui, *Nanoscale*, 2015, **7**, 1363-1373.